NIF

DOE/NASA/10769-10
NASA TM-82 ~~82~~ 673

82673

High B-Field, Large Area Ratio MHD Duct Experiments

J. Marlin Smith, Shih-Ying Wang, and J. L. Morgan
National Aeronautics and Space Administration
Lewis Research Center

Work performed for
U.S. DEPARTMENT OF ENERGY
Fossil Energy
Office of Magnetohyrodynamics

Prepared for
International Conference on Plasma Science
Institute of Electrical and Electronics Engineers
Santa Fe, New Mexico, May 18-20, 1981

NOTICE

DOE/NASA/10769-19
NASA TM-82673

High B-Field, Large Area Ratio MHD Duct Experiments

J. Marlin Smith, Shih-Ying Wang, and J. L. Morgan
National Aeronautics and Space Administration
Lewis Research Center
Cleveland, Ohio 44135

Work performed for
U.S. DEPARTMENT OF ENERGY
Fossil Energy
Office of Magnetohydrodynamics
Washington, D.C. 20545
Under Interagency Agreement DE-AI01-77ET10769

International Conference on Plasma Science
sponsored by the Institute of Electrical and Electronics Engineers
Santa Fe, New Mexico, May 18-20, 1981

E-956

HIGH B-FIELD, LARGE AREA RATIO MHD DUCT EXPERIMENTS

J. Marlin Smith, Shih-Ying Wang, and J. L. Morgan

National Aeronautics and Space Administration
Lewis Research Center
Cleveland, Ohio 44135

INTRODUCTION

Combustion-driven magnetohydrodynamic (MHD) generators show great promise for various electrical power generation applications. The Lewis Research Center (LeRC) has in operation a small (4-12 MW_T) cesium-seeded H_2-O_2 combustion MHD generator to investigate performance and fluid dynamics at high magnetic field levels. The MHD power generation experiments are conducted in a high field strength, liquid neon cooled cryomagnet (fig. 1 and ref. 1). In this facility, a peak field of ≥ 6 tesla should be obtainable. The time duration of the experiment is limited by the neon supply which allows on the order of a few minutes of total operating time followed by an 18-hour reliquefaction period. As a result, the experiments are run with heat sink MHD hardware in a pulsed mode. The run duration for the data presented here was 5 sec.

Experiments have been carried out using a diverging area Hall duct having an entrance Mach number of 2. In these experiments, the Hall configuration was chosen over the more efficient Faraday or diagonal wall (DW) configurations due to its simplicity of construction. In our initial experiments (ref. 1), a conically bored duct with an overall area ratio of 2.56 was used. The effects of power takeoff location, generator loading, B-field strength, and electrode breakdown voltage were investigated. The significant results of this testing were the linear increase in power output of the generator with the square of the B-field and the observation of interelectrode electrical breakdown resulting from jxB forces which forced the anode electric current into the interelectrode insulators at electrical stresses above approximately 50 volts/insulator.

As a result of these experiments and subsequent theoretical analysis, it was established that a further increase in performance could be achieved with a duct of larger area ratio, by multiple loading of the duct, and by relocating the duct within the magnetic field. For this second series of experiments (ref. 2), the generator duct was conically bored to an area ratio of 4. The linear increase in power output with B^2 was still observed, and the power output increased from greater than 100 percent at low B-field to approximately 50 percent at high B-field. Relocation of the duct within the magnetic field indicated that additional power could be generated using a longer duct.

On the basis of the above results and principally due to the fact that the duct was limited by design constraints to a maximum area ratio of 4, a new Hall duct was constructed. This duct allows a maximum area ratio of 6.25, is approximately 20 percent longer, and has a segmentation pitch one-half the size of the original duct. Three series of tests have been performed with this duct having area ratios of 4, 5, and 6.25, respectively. Test data at an area ratio of 4 substantially agreed with that obtained in the original duct at this area ratio. At an area ratio of 5, the power output remained linear with B^2 and the maximum power output increased by approximately 30 percent. However, at an area ratio

of 6.25, the power no longer increased with B^2, rising less rapidly at higher B-fields. This is the result of the choking of the channel which is seen from axial pressure profiles to move upstream with increasing B-field. This effect was also observed at low combustion pressures for the 4/1 area ratio duct (ref. 2).

EXPERIMENTAL FACILITY AND CONFIGURATION

The experimental facility has been discussed in detail previously (refs. 1 to 3) and therefore will be discussed only briefly in this paper. The facility consists of a liquid neon cooled cryomagnet with a 23.5 cm (9-1/4 inch) bore tube into which a rocket-type gaseous O_2-H_2 combustor, MHD duct, and diffuser are inserted (fig. 1). The MHD power train is electrically isolated from ground all the way from the supply lines to the combustor, out to the electrically isolated sump tank and stack. The combustor is capable of operating over a wide range of pressure and oxygen/hydrogen ratios. The nominal conditions are 10 atm and an oxygen/hydrogen weight ratio of 8. The cesium seed is injected into the oxygen supply line as a 75 percent solution by weight of CSOH dissolved in water. Upon exiting the diffuser, the H-O-Cs exhaust gases are cooled and condensed by water injection which then flows to a sump for recirculation. With the exception of the MHD duct and diffuser, which are of heat sink design, the facility is capable of steady-state operation within the time limitation of the neon supply. Since the present limit of this supply only allows continuous running for the order of a few minutes followed by an 18-hour reliquefaction period, it was decided to operate the facility in a pulsed mode which allows the simplicity of heat sink MHD hardware. The construction of the hardware was further simplified by using a Hall duct configuration.

In figure 2, the MHD duct location relative to the axial magnetic field profile is shown. It is seen that the center point of the duct corresponds to the centerline of the magnetic field profile. Also shown is the approximate location of the power takeoff leads which, for the 4/1 and 5/1 area ratio ducts, were electrodes 36, 37, 38 and electrodes 90, 91, 92, while for the 6.25/1 area radio duct the front power takeoff electrodes were 38, 39, 40. The reason that the whole duct cannot be used is shown in figure 3 in which the Hall voltage is plotted versus electrode number, i.e., distance down the duct. In run 100, the power takeoff was from electrodes 1, 2, 3 to the diffuser. It is seen that in the region extending from the front power takeoff region to approximately the 30th electrode, the voltage gradient is negative indicating that the region is one of power dissipation rather than power generation. This is due to the fact that insufficient voltage is being generated in this region to pass the current generated by the duct as a whole. A similar situation occurs to a minor extent at the rear of the duct. In order to achieve maximum power output with a single load resistance, the power takeoff locations should be located at the front and rear inflection points of the Hall voltage versus electrode number curve as is shown in the curve for run 147. It is seen that the power output is increased by a factor of greater than 50 percent by this optimal location of the power takeoff leads. A more thorough discussion of the effect of power takeoff location and the effect of multiple loading of the duct is presented in references 2 and 3.

Also seen from figure 2 is that the magnetic field varies appreciably over the active length of the duct going from approximately 90 to 45 percent of peak field from the front to the rear power takeoff regions, respectively. Therefore, references to the operating magnetic field strength of the duct are to the peak field values.

MHD DUCT CONSTRUCTION

The original duct used in the 2.56/1 and 4/1 area ratio experiments is shown on the top half of figure 4. It basically consisted of four modules made up of eight circular electrodes clamped together by two triangular-shaped end plates. The alignment of the module was maintained by three fiberglas rods. This ten-electrode module has a segmentation pitch of 1.38 cm. The four modules are bolted together and two 2.22 cm triangular end plates are added to provide sufficient thickness for bolting to the combustor, nozzle and diffuser. The duct therefore consisted of 42 electrodes. A picture of this duct is shown in figure 5, and other details of the design are given in reference 1.

In the original duct, the area ratio was limited to a maximum of 4/1 mainly due to the temperature limitation on the fiberglas alignment rods and the surface available for the interelectrode gaskets. In the new design, this problem was overcome by rotating the alignment rods 60 degrees relative to the tie rod holes, increasing the outer diameter of the circular electrodes from 15.2 cm to 17.8 cm, and rounding the sides of the triangular plates out to the edge of the 17.8 cm diameter circular electrodes as shown in the drawing on the lower half of figure 4. Also in order to reduce the possibility of interelectrode electrical breakdown, the segmentation pitch was reduced to 0.74 cm. The duct was then made up of five modules consisting of 16 circular electrodes clamped by three electrically isolated stainless steel tie bolts between two triangular electrodes at each end for a total of 20 electrodes/module. The copper electrodes are 0.64 cm wide and electrically insulated from one another by a high-temperature asbestos gasket 0.078 cm thick (to provide the pressure seal), sandwiched between two 0.013 cm thick sheets of mica (to provide the electrical insulation and moisture barrier). Lateral movement of the electrodes is negated by three fiberglas rods inserted through the entire module. Five such modules are used in the present experiments with 2.22 cm thick end flanges for a total of 102 electrodes having a total length of approximately 78 cm. Figure 6 is a picture of the combustor-generator-diffuser assembly.

EFFECT OF AREA RATIO ON POWER OUTPUT

One of the interesting results observed in early experiments was the linear increase in the power output with the square of the B-field. This observation is reproduced from reference 2 in figure 7 for the previous tests at area ratios of 2.56/1 and 4/1. For clarity, the data points associated with these curves are not reproduced. Tests with the new duct at an area ratio of 4/1 were identical to the previous test at this area ratio. At an area ratio of 5/1, the linear dependence on the square of the B-field was still observed as shown by the circular data points and a peak power output of $\simeq$170 kW at a magnetic field strength of 5 tesla was obtained. Upon increasing the area ratio to 6.25/1, the linear increase in power output with the square of the B-field persisted up to

a magnetic field strength of approximately 3 tesla at which point the increase in power output decreased significantly, falling below that of the 5/1 area ratio duct and producing about the same power output as the 4/1 area ratio duct at 5 tesla. The data points for the 6.25/1 area ratio duct are shown by the diamond shaped points in figure 7.

The reason for the decreased performance of the 6.25/1 area ratio duct is shown in figure 8 in which the static pressure in the duct is plotted as a function of electrode number, i.e., distance down the duct. Up to a magnetic field strength of approximately 3.5 tesla, the pressure distribution is seen to monotonically decrease with distance down the duct as shown by the circular data points. At higher magnetic field strengths, e.g., 4 and 5 tesla, an abrupt discontinuity in the pressure distribution is observed upstream of the exit of the duct. This discontinuity represents a shock in the duct which moves upstream with increasing enthalpy extraction, i.e., increasing magnetic field strength. These shocks have a profound influence upon the power that can be extracted from the channel, since in the region downstream of the shock, the flow is subsonic and the reduced velocity results in a decrease in the generated voltage.

The formation of shocks with the resulting decrease in the rate of increase in power output with magnetic field was previously observed in the 4/1 area ratio channel at a combustion pressure of 100 psia (ref. 2). From this previous result and the results of the present tests at a combustion pressure of 150 psia, it is clear that for a given combustion pressure there is a duct area ratio below which there is no shock formation, and the power output increases with the square of the magnetic field. By increasing the combustion pressure, the shocks are pushed downstream and the area ratio below which the duct will operate shock free can be increased with a subsequent increase in the performance of the duct. The performance increase will occur up to the point at which the electrical conductivity decrease due to the pressure increase in the upstream portion of the duct (fixed inlet area) overcomes the beneficial influence of the area ratio increase. These results are shown in figure 9 in which the power output is shown as a function of the square of the magnetic field for various combustion pressures. At a combustion pressure of 100 psia, the performance of the duct is considerably less than that at the higher combustion pressures and even appears to be approaching an asymptotic limit of approximately 30 kW with increasing magnetic field strength. As seen from figure 10, this poor performance is a result of an even stronger shock wave structure than previously observed at 150 psia (fig. 8) with a shock being present in the duct even with no magnetic field as shown by the circular data points. At a magnetic field strength of 4.5 tesla, the shock has moved upstream to approximately the 32nd electrode which is now upstream of the upstream power takeoff electrodes 38-40 so that the power generation region of the duct is operating entirely subsonic. As the combustion pressure is increased to 150 psia, the shock is pushed downstream (compare figs. 8 and 10), and a significant increase in duct performance is obtained as shown in figure 9. However, as previously noted the performance at magnetic fields above ≈3 tesla is still reduced by the presence of a shock in the duct. As the combustion pressure is further increased to 175 psia, the shock is pushed completely downstream of the power generation region of the duct, and the linear increase in power output with the square of the magnetic field is seen to exist again as shown by the square data points in fig-

ure 9. However, as is obvious from the comparison of the 150 and 175 psia curves, the performance at 175 psia is less than that of the 150 psia case in the shock-free region due to its lower electrical conductivity, but eventually exceeds the power output of the 150 psia case as the linear increase in power output at 150 psia is reduced by the presence of a shock within the duct at the higher magnetic fields.

CONCLUDING REMARKS

Studies of the effect of area ratio variation on the performance of a supersonic Hall MHD duct have been extended to area ratios of 6.25/1 from the previous limit of 4/1 by the design and construction of a new duct. It has been shown that for a given combustion pressure there exists an area ratio below which the power generating region of the duct is shock free. In this shock-free regime, the power output of the duct is found to increase linearly with the square of the magnetic field. For area ratios greater than this, a shock forms in the power generating region which moves upstream with increasing magnetic field strength resulting in a less rapid rise in the power output. Increasing the combustion pressure moves the shock back downstream and results in an increase in the performance of the duct up to a point where the decrease in electrical conductivity due to the increased pressure at the upstream end of the duct (fixed inlet area) overcomes the increase in power output due to the area ratio increase.

The peak performance of the duct occurred at an area ratio of 5/1 for a combustion pressure of 150 psia. For this condition, 180 kW was generated which represents a 2.5 percent enthalpy extraction. For the next series of tests, a vacuum exhaust system has been installed which will allow the shocks to be removed from the power generating region of the duct at lower combustion pressures. It is anticipated that shock-free operation can be accomplished at combustion pressure below 100 psia which will result in enthalpy extractions of the order of 4 percent.

REFERENCES

1. J. M. Smith, "Preliminary Results in the NASA Lewis H_2-O_2 Combustion MHD Experiment," in 18th Symposium on the Engineering Aspects of Magnetohydrodynamics, Montana State Univ., Bozeman, MT, 1979, pp. A.2.1-A.2.6.
2. J. M. Smith, "Results of Duct Area Ratio Changes in the NASA Lewis H -O_2 Combustion MHD Experiment," Presented at the AIAA Eighteenth Aerospace Sciences Meeting, Pasadena, CA, January 14-16, 1980, AIAA Paper 80-0023.
3. J. M. Smith, "Experiments on H_2-O_2 MHD Power Generation," Presented at the Third World Hydrogen Energy Conference, Tokyo, Japan, June 23-26, 1980.

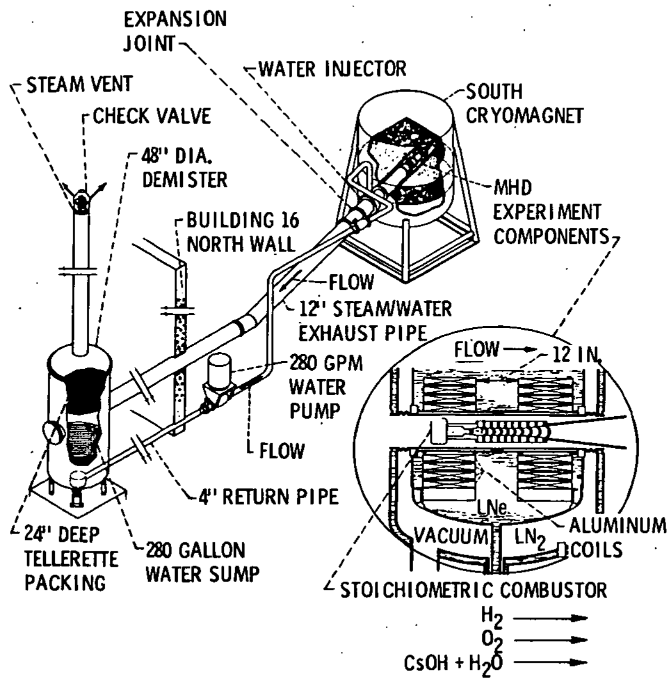

Figure 1. - GH_2-GO_2 combustion MHD experiment installation.

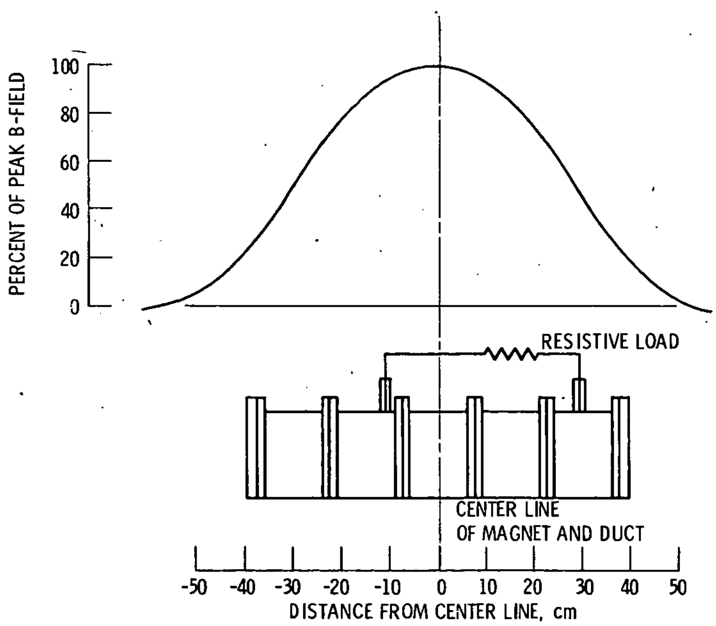

Figure 2. - Duct location within magnetic field.

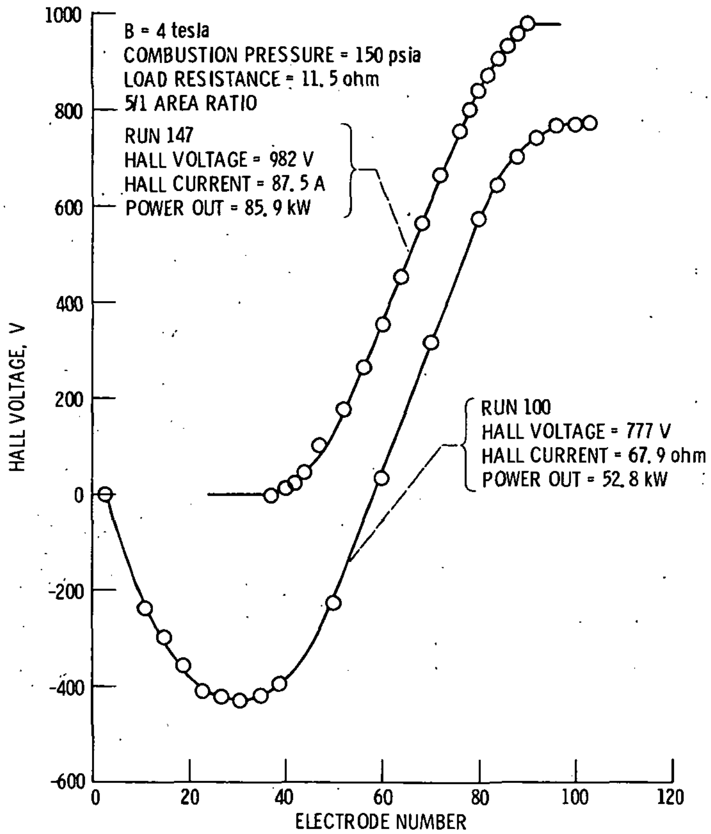

Figure 3. - Effect of power takeoff location upon generator performance.

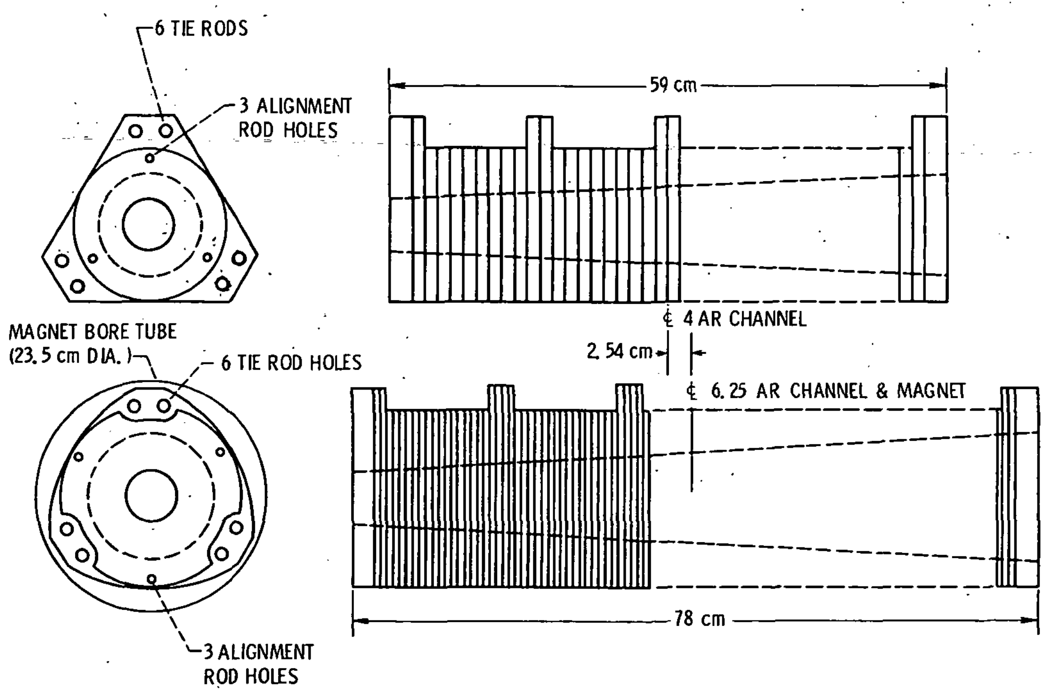

Figure 4. - Comparison of construction between 1.38 and 0.69 cm segmentation ducts.

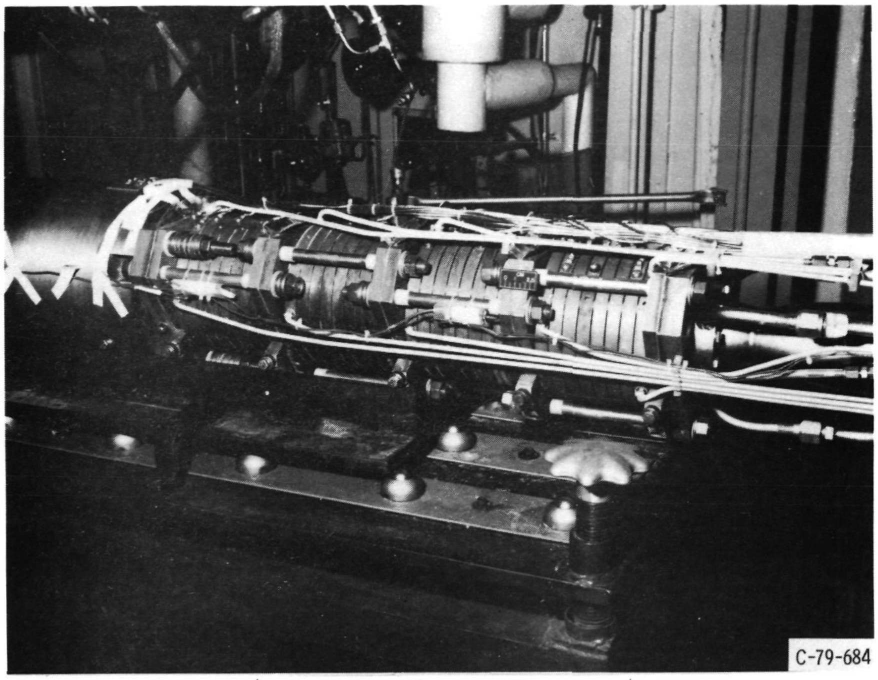

Figure 5. - 1.38 Segmentation ratio duct.

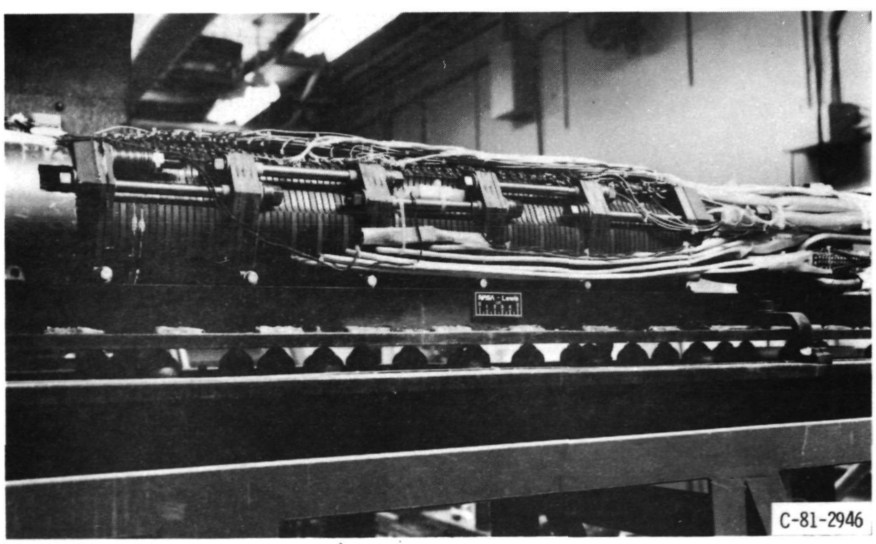

Figure 6. - 0.69 Segmentation ratio duct.

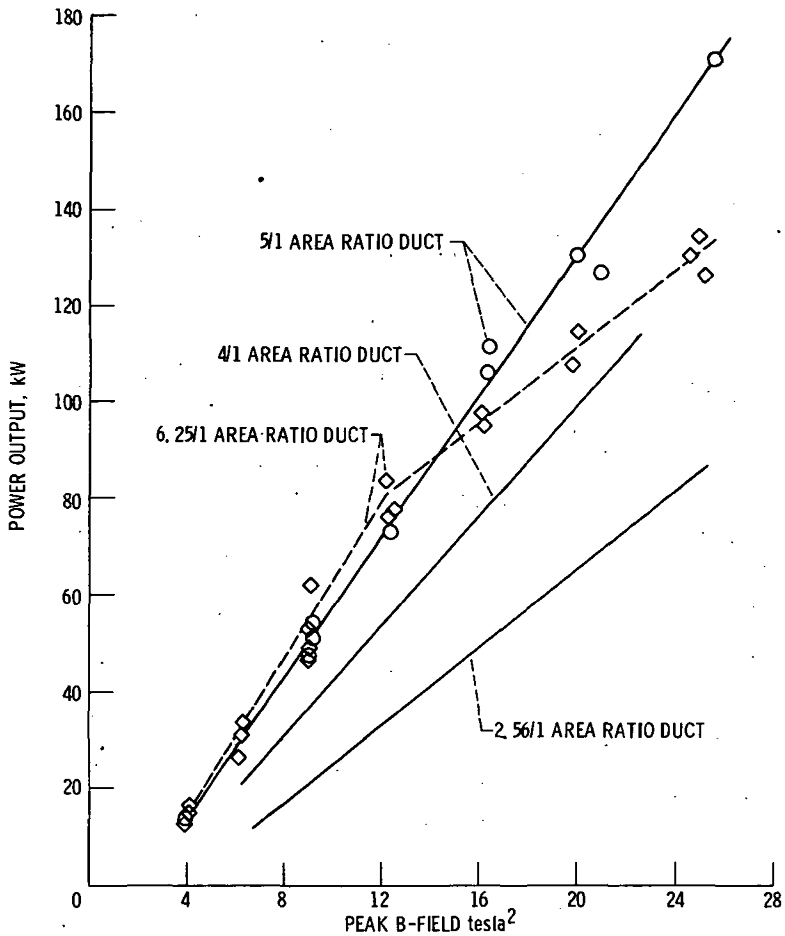

Figure 7. - Power output versus B-field squared as a function of duct area ratio for P_c = 150 psia.

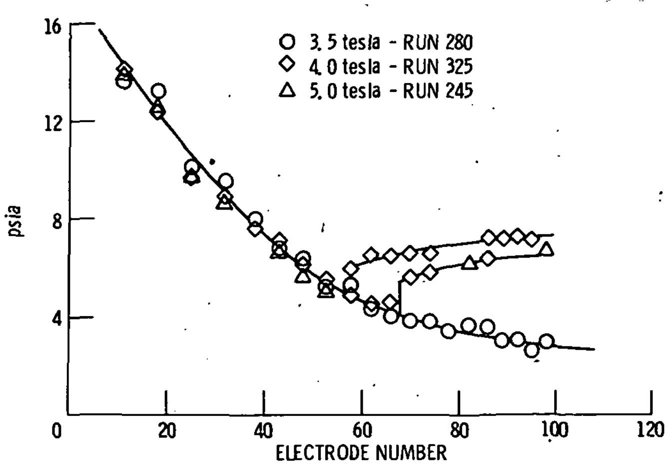

Figure 8. - Axial pressure distribution for an AR = 6.25 and P_c = 150 psia as a function of B-field.

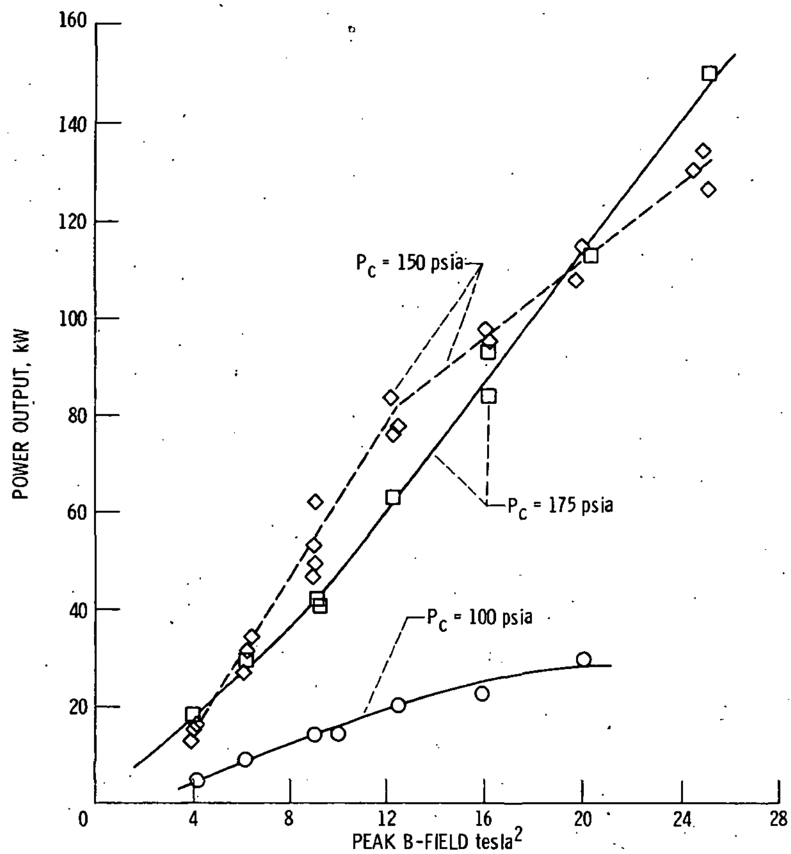

Figure 9. - Power output versus B-field squared as a function of combustor pressure for area ratio = 6.25.

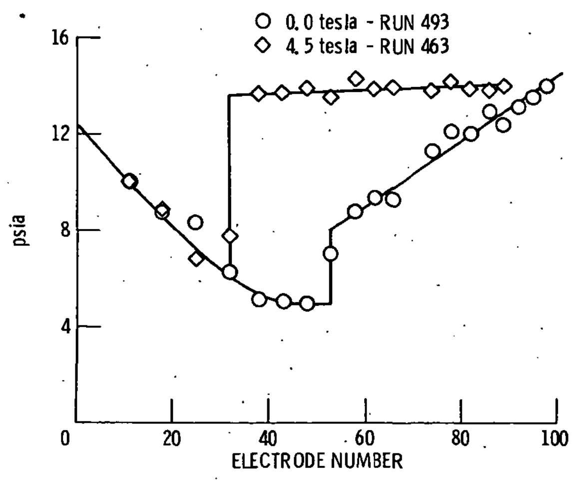

Figure 10. - Axial pressure distribution for an AR = 6.25 and P_c = 100 psia as a function of B-field.

1. Report No. NASA TM-82673	2. Government Accession No.	3. Recipient's Catalog No.
4. Title and Subtitle HIGH B-FIELD, LARGE AREA RATIO MHD DUCT EXPERIMENTS		5. Report Date
		6. Performing Organization Code 778-11-05
7. Author(s) J. Marlin Smith, Shih-Ying Wang, and J. L. Morgan		8. Performing Organization Report No. E-956
9. Performing Organization Name and Address National Aeronautics and Space Administration Lewis Research Center Cleveland, Ohio 44135		10. Work Unit No.
		11. Contract or Grant No.
		13. Type of Report and Period Covered Technical Memorandum
12. Sponsoring Agency Name and Address U.S. Department of Energy Office of Magnetohydrodynamics Washington, D.C. 20545		14. Sponsoring Agency ~~Code~~ Report No. DOE/NASA/10769-19

15. Supplementary Notes

Prepared under Interagency Agreement DE-AI01-77ET10769. Prepared for International Conference on Plasma Science sponsored by the Institute of Electrical and Electronics Engineers, Santa Fe, New Mexico, May 18-20, 1981.

16. Abstract

Studies of the effect of area ratio variation on the performance of a supersonic Hall MHD duct have been extended up to area ratios of 6.25/1. It is shown that for a given area ratio there is a combustion pressure above which the power generating region of the duct is shock free and the power output increases linearly with the square of the magnetic field. Below this pressure a shock forms in the duct which moves upstream with increasing magnetic field strength and results in a less rapid rise in power output.

17. Key Words (Suggested by Author(s))	18. Distribution Statement
Magnetohydrodynamics Power generation Fluid dynamics	Unclassified - unlimited STAR Category 75 DOE Category UC-90g

19. Security Classif. (of this report)	20. Security Classif. (of this page)	21. No. of Pages	22. Price*
Unclassified	Unclassified		

* For sale by the National Technical Information Service, Springfield, Virginia 22161